COMMISSION A:
Electromagnetic Metrology, Electromagnetic measurements and standards
(November 2020 – May 2023)

Edited by

Hidekazu Hachisu (National Institute of Information and Communications Technology; NICT)

A1. Time and Frequency Standards and Time Transfer Technique

The research and development on time and frequency standards as well as time and frequency transfer in Japan are mainly carried out at the National Metrology Institute of Japan (NMIJ) and the National Institute of Information and Communications Technology (NICT).

At NMIJ, the second cesium fountain, NMIJ-F2, for primary frequency standards has been developed. We evaluated the frequency shifts due to the microwave leakage and distributed cavity phase. By measuring the frequency of NMIJ-F2 as a function of the microwave pulse area, the frequency correction and uncertainty for the microwave leakage shift were evaluated to be $(-1.2 \pm 2.5) \times 10^{-16}$. Furthermore, by measuring the frequency of NMIJ-F2 with changes of the tilt angle of the fountain, the frequency correction and uncertainty for the distributed cavity phase shift were evaluated to be $(0 \pm 3.4) \times 10^{-16}$. By these, the uncertainty evaluation of NMIJ-F2 was completed [1]. The type A uncertainty for measurement for 20 d and the type B uncertainty are typically 1.7×10^{-16} and 4.6×10^{-16}, respectively. Ultrastable microwave oscillators: We have developed three cryo-refrigerator-cooled cryogenic sapphire-resonator oscillators (cryoCSOs) with a frequency stability of an order of 10^{-15} at an averaging time of 1 s. One of them is continuously operating, except during an annual scheduled power outage due to an inspection of electrical facilities and works as a local oscillator of the cesium fountain NMIJ-F2.

At present two active hydrogen maser frequency standards are operated at NMIJ for time keeping. Those atomic clocks are kept in individual chambers, whose temperature variations are kept to within 0.2 deg C. One of the hydrogen masers is used as a source oscillator for generating UTC(NMIJ), which is created by frequency-steering of the hydrogen maser output signal using a frequency stepper (AOG). At NMIJ, Dual frequency carrier phase GPS receiver is one of the main international time and frequency transfer tools. NMIJ has been providing the remote frequency calibration service using the GPS common-view method and Internet since 2006. The CMCs of the service are 1.1×10^{-13} (baseline: 50 km), 1.4×10^{-13} (baseline: 500 km) and 4.9×10^{-13} (baseline: 1,600 km) at an averaging time of one day. The number of users is 18 in 2023.

NICT maintains Japan Standard Time (JST) and disseminates it domestically. From November

2020 to May 2023, the difference between the Coordinated Universal Time (UTC) and UTC(NICT) has been kept within 20 nanoseconds. Since August 2021 NICT's strontium optical lattice clock NICT-Sr1 is used as an additional reference, remarkably reducing the difference to within 5 nanoseconds, a quarter of the previous difference. Throughout the period, NICT's Kobe JST substation has continued to keep the standard time, which is constantly monitored and steered by the distributed and integrated management of JST stations. Kobe substation operates as an emergency backup station for the Tokyo headquarters.

Regarding the next-generation TWSTFT modem (SRS modem), NICT conducted time and frequency (T&F) transfer experiments with national metrology institutes of three European countries, the Physikalisch-Technische Bundesanstalt (PTB) in Germany, the Observatoire de Paris (OP) in France, and the Istituto Nazionale di Ricerca Metrologica (INRiM) in Italy, and reported its results at international meetings including the CCTF (Consultative Committee for Time and Frequency) working group. Starting 2022, a collaboration contract has been concluded among the Research Institute of Sweden (RISE) in Sweden and the above three national metrology institutes, and a T&F transfer experiment with SRS modems within the European region is being planned. Domestically, a regular time comparison link among four stations (two low frequency (LF) Stations, Kobe substation, and Koganei headquarters) has been constructed using the SRS modem. Frequency comparison using a global navigation satellite system (GNSS) precise point positioning (PPP) method was started among NICT, MMIJ, and the Korea Research Institute of Standards and Science (KRISS) to realize regular mutual comparison of their optical frequency standards. NICT started nearly-real-time time comparison using the augmentation service MADOCA-PPP broadcast by Michibiki (Quasi-Zenith Satellite System) in order to increase the accuracy and robustness of the time comparison link used in the decentralization of JST. It was confirmed that almost the same accuracy can be obtained as using satellite orbit information provided by the International GNSS Service (IGS) with a delay of several hours. Participating in the "Task Force GNSS Traceability" established under the CCTF GNSS WG in June 2020, the results of the discussions were published in [2].

Wireless two-way interferometry (Wi-Wi) developed at NICT was applied to low latency communication [3-5], to physical layer security [6] and to automatic mobility following [7].

Considering the cost reduction and mass production of miniaturized atomic frequency standards, NICT developed a GHz-band MEMS oscillator using a legacy process (line width of 150 nm or more), and a VCSEL with MEMS wavelength tuner [8]. In addition, for wafer-level fabrication of gas cells, NICT successfully synthesized a solid Rb source (RbN_3) that does not generate reaction products undesired for wafer processes [9]. To transfer these technologies to companies in the future, a joint research program with companies and universities has been started. To reduce the size of the physics package further, NICT started developing the laser handling

techniques for the atomic clock, such as steering, polarization, or collimation, using metasurface patterns [10].

NICT has started development of a distributed time synchronization system utilizing small atomic clocks to construct a resilient time synchronization network. Simulations using a state-space model of small atomic clocks were performed to investigate the effect of network topology, connection method and number of atomic clocks on the stability of timescale generation using a Kalman filter in a network of multiple atomic clocks [11].

The redefinition of the SI second requires the stable operation of optical atomic clocks, and so it is important to understand frequency changes caused by solid-earth tides that often range from 10 to 20 cm in amplitude, by oceanic tidal loading, crustal deformations due to earthquakes, and ground movements with groundwater changes. NICT has begun observations and data analysis to evaluate how these effects interact with optical atomic clocks [12]. Since early 2021, NICT and the Geospatial Information Authority of Japan (GSI) have been jointly conducting leveling surveys and relative gravimeter observations at the NICT's headquarters in Koganei. These observations reduce the contribution of gravitational redshift to the total uncertainty of NICT-Sr1 to the 10^{-19} level. With the support of the National Institute of Polar Research (NIPR), absolute gravity measurements were performed in August 2019 and May 2022 to evaluate the effects of the 2011 off the Pacific coast of Tohoku Earthquake on coseismic vertical crustal displacement. The obtained absolute gravity change between the two periods was −43.8 μGal. This matches the trend of GNSS results obtained by the GNSS Earth Observation Network system (GEONET) of GSI, which show a vertical displacement of up to 31.5 mm from August 2019 to May 2022 (equivalent to about −10 μGal gravity change) even though the values do not agree precisely. NICT has introduced the Micro-g LaCoste's gPhoneX gravimeter for continuous gravity measurements near the optical clocks at the end of 2021. The preliminary results over seven months detect stable gravity change due to solid earth tide with about 22 μGal precision. NICT is also monitoring vertical crustal displacement by geodetic GNSS measurement.

[References]

[1] A. Takamizawa, S. Yanagimachi, and K. Hagimoto, "First uncertainty evaluation of the cesium fountain primary frequency standard NMIJ-F2," Metrologia **59**(3), 035004 (2022).

[2] P. Defraigne, J. Achkar, M. J. Coleman, M. Gertsvolf, R. Ichikawa, J. Levine, P. Uhrich, P. Whibberley, M. Wouters, and A. Bauch, "Achieving traceability to UTC through GNSS measurements," Metrologia **59**, 064001 (2022).

[3] D. Koyama, Y. Wang, N. Shiga, S. Yasuda, N. Chauvet, and M. Naruse, "Low latency information transfer based on precision time synchronization via wireless interferometry, "Nonlinear Theory and Its Applications, IEICE **12**, 2, 225–235 (2021).

[4] Y. Yamasaki, N. Chauvet, N. Shiga, S. Yasuda, K. Takizawa, R. Horisaki, and M. Naruse, "Delay-bounded Wireless Network Based on Precise Time Synchronization Using Wireless Two-way Interferometry," IEEE Access **9**, 85084 (2021).

[5] H. Tanaka, Y. Yamasaki, S. Yasuda, N. Shiga, K. Takizawa, N. Chauvet, R. Horisaki, and M. Naruse, "Experimental Demonstration of Delay-Bounded Wireless Network Based on Precise Time Synchronization," IEEE Access **10**, 94285 (2022).

[6] N. Shiga, S. Yasuda, K. Yonaga, K. Takizawa, M. Yoshida, "Virtual Wiretap Channel Based on Wireless Two-way Interferometry," in Proc. the 2022 IEEE Global Communications Conference (GLOBECOM 2022), 6188 (2022).

[7] R. Isogai, S. Yasuda, N. Shiga, Y. Shoji, "Extremely High-accuracy Automatic Following between Mobilities Using Wireless Two-way Interferometry," in Proc. 2023 IEEE 20th Consumer Communications & Networking Conference (CCNC), 829, (2023).

[8] M. Hara, S. Shinada, Y. Yano, T. Ido, Z. Zhao, M. Toda, T. Ono, and H. Ito, “FBAR Oscillator and MEMS Tunable VCSEL to Generate the Probe Lasers for Microfabricated Atomic Clock”, in Proc. 2022 IEEE International Ultrasonics Symposium (IUS), 1-4 (2022).

[9] M. Hara, Y. Yano, M. Toda, T. Ono, and T. Ido, “Evaluation of New Solid Rubidium Source Using Atomic Clock Stabilization Loop”, in Proc. 2021 21st International Conference on Solid-State Sensors, Actuators and Microsystems (Transducers), 1158-1161 (2021).

[10] P. Prutphongs, K. Aoki, S. Ikezawa, M. Hara, and K. Iwami, “Multifunctional Metasurface for a Miniaturized Reflection-type Atomic Vapor Cell”, in Proc. 2023 22nd International Conference on Solid-State Sensors, Actuators and Microsystems (Transducers), (in Press).

[11] Y. Yano, M. Hara, and I. Ido, “Time Estimation of a Miniature Atomic Clock Using Instantaneous Frequency Information,” URSI Radio Science Letters **4**, 48 (2023).

[12] R. Ichikawa, H. Hachisu, M. Sekido, T. Ido, Y. Hiraoka, E. Harima, S. Fukaya, K. Matsuo, M. Nakashima, Y. Aoyama, A. Hattori, and Y. Fukuda, “Geodetic measurements and quantitative evaluation for reduced gravitational redshift uncertainty of NICT optical frequency standards,” IFCS-EFTF 2023, in Proc. 2023 Joint Conference of the IEEE International Frequency Control Symposium and the European Frequency and Time Forum (IEEE IFCS-EFTF 2023) (in press).

A2. Laser Stabilization & Frequency Measurement

Several institutes in Japan conduct research and development on laser stabilization and frequency measurement.

NICT's strontium optical lattice clock NICT-Sr1 is recognized as a secondary frequency standard since 2018. An updated evaluation of its frequency against remote primary standards was reported in 2021, with an uncertainty of 1.8×10^{-16} [1]. NICT began the continuous generation of an optically steered, physical timescale signal in July 2021, using NICT-Sr1 to determine adjustments to the frequency of an active hydrogen maser [2]. From August 2021, this timescale is referenced in the generation of JST, which has reduced its deviation from UTC [3]. NICT-Sr1 also contributed calibration data for the interval of International Atomic Time (TAI) each month from August 2021 to August 2022. NICT has established a collaboration with NMIJ and KRISS to share measurement results of the optical lattice clocks at these institutes. Data is exchanged in terms of frequency evaluations for hydrogen masers and the local realization of UTC at each institute with respect to their optical lattice clocks, combined with comparisons of these local UTC realizations by the GNSS PPP technique.

At NICT, an In^+ frequency standard based on sympathetic cooling with Ca^+ is in development, and in 2020 the frequency ratio of In^+/Sr was measured with a fractional uncertainty of 7.7×10^{-16} [4]. The major contribution to the uncertainty comes from the evaluation of micro- and secular-motion of the In^+. A new approach replacing Ca^+ with Yb^+ for sympathetic cooling is in progress to reduce the mass ratio from 3 to 1.5 for better control of the In^+ motion.

NICT is developing frequency standards in the THz region. A 3.1 THz quantum-cascade laser was stabilized to $J = 27-26$ rotational transition of CO molecules and the uncertainty was evaluated to be 3.6×10^{-8}. A portable 0.3 THz standard based on the difference-frequency generation of two C_2H_2-stabilized 1.5 μm lasers was developed simultaneously, with an uncertainty of 4.5×10^{-8}. A theoretical study on the possibility of the precision measurement of vibrational-rotational transition frequencies in the THz region was presented for the HeH^+, NeH^+, and ArH^+ molecular ions, with an expected uncertainty of 10^{-15} [5]. In further work, a high-precision THz counter with wide measurable bandwidth was developed using a semiconductor-superlattice harmonic mixer, attaining an uncertainty below 1×10^{-16} over 4 octaves from 0.1 THz to 3 THz [6].

At NMIJ, the Yb optical lattice clock NMIJ-Yb1 participated in the on-time calibration of international atomic time for 13 months during the period 2021-2023, with an operating period of 5 - 30 days per month and an availability rate of more than 80%. Particularly high availability rates of 94.5% for 30 days in August 2021 and 97.0% for 20 days in March 2022 were achieved. In addition, the Yb optical lattice clock NMIJ-Yb1 is routinely compared with the Cs fountain clock NMIJ-F2, and a dark matter search was conducted using the data from 2020-2021. The

results show that in the very low mass region (10^{-22} - 10^{-21} eV), the coupling constants between dark matter and electrons are more strongly constrained than in previous studies [7]. In addition, the comparison uncertainty with UTC using the optical frequency comb could become a bottleneck due to the higher accuracy of NMIJ's ^{171}Yb optical lattice clock. To overcome this problem, the comparison accuracy between UTC and optical lattice clocks was improved to 4 × 10^{-18} by improving the precision of the system that frequency synthesizes the frep of the optical frequency comb from 10 MHz of UTC(NMIJ) [8].

Katori group at the University of Tokyo and RIKEN is developing a transportable optical lattice clock [9] for applications in relativistic geodesy [10, 11]. The entire setup, including lasers, optics, electronics, and physics package, has a volume of 250 L (27% of existing systems) and a weight of 150 kg (40%), making it the most compact clock system with a target uncertainty of ~10^{-18}. They also propose a scheme of longitudinal Ramsey spectroscopy that allows continuous interrogation of atoms in the lattice to improve the instability of the clock by $\sigma \propto 1/\tau$ [12]. They have succeeded in continuously extracting atoms from the magneto-optical trap with moving lattice [13]. They started developing a nuclear clock based on the low-energy nuclear transition of thorium-229 (Th-229). The nuclear clock is expected to achieve unprecedented accuracy because the resonance frequency of the nuclear transition is thought to be insusceptible to the fluctuations of the environment due to the shielding by the surrounding electron shells. Toward a nuclear clock, they trapped triply charged Th-229 ions and performed laser spectroscopy. They also trapped Th-229 ions in the isomer state (the nuclear-excited state at 8.3 eV) and determined its nuclear properties by measuring the hyperfine constants [14].

Hong group at Yokohama National University is developing optical frequency combs and frequency stabilized lasers. They have developed a low-repetition-rate dual comb spectrometer for molecular spectroscopy at visible wavelengths [15]. They have also developed a 3D Yb magneto-optical trap using a dispenser atomic source [16] and an iodine-stabilized laser at 556 nm for Yb cold atom experiments [17]. They also performed laser frequency measurement in the short-wavelength region using an intermediate laser and a frequency noise cancellation method [18].

Sugiyama group at Kyoto University has been developing Yb^+ and Ba^+ ion clocks. The group aims at search for a temporal variation of the fine-structure constant and precise measurement of isotope shifts. Three-dimensional cooling technique has been established and the second trap system is being developed for Yb^+ ions [19]. Optical frequency-ratio measurement systems has been developed using octave-spanning optical frequency combs based on a mode-locked ytterbium-doped potassium-yttrium-tungstate (Yb:KYW) laser [20].

Nakagawa group at University of Electro-Communications (UEC) have developed

transportable atomic gravimeters based on cold Rb atoms for the field applications under the national quantum technologies program. The transportable atomic gravimeters are required for the precision gravity measurements in the fields of geophysics, metrology, and navigation. We developed a compact sensor head (a height of 60 cm and a diameter of 24 cm) and a transportable laser system for the atomic gravimeter based on telecom lasers and fiber optics [21]. We achieved a sensitivity of 1.5×10^{-8} g for the integration time of 1000 s [22].

Musha group at UEC has been developing space-borne photonic microwave frequency references for the next-generation Japanese quasi-zenith satellite in which the frequency of a frequency-stabilized light source is down-converted to the microwave region by using an optical frequency comb. As an optical frequency reference, the frequency of 3rd harmonics of a 1545-nm ECLD is stabilized in reference to the saturated absorption of iodine molecule at 515 nm. The frequency stability of this laser is evaluated by using the H-maser-locked optical frequency comb at NICT, and it reaches 8×10^{-15} at 1000 s. This frequency-stabilized light source will be also utilized for the light source of Japanese space gravitational wave detector DECIGO. The NALM-type figure-8 Er mode-lock fiber laser around 1.5 μm has been also developed for the optical frequency comb, and self-starting of the mode-lock operation and low phase noise are achieved which has been hardly obtained in the conventional figure-8 fiber mode-lock lasers. Our fiber mode-lock lasers passed the disturbance and the thermal vacuum tests which shows their high robustness as the space-borne laser. For the formation flying of multiple satellites in space which is indispensable technique for DECIGO project, we propose and develop the 3-dimentional satellite position tracking system which consists of single-frequency laser and acousto-optic deflector (AOD). Our system has the angle resolution of 2 micro radian and length resolution of 2 m, and now plan to install it on a small engineering test satellite for the precision formation flying in space.

Goka group at Tokyo Metropolitan University (TMU) is developing chip-scale atomic clocks. They have developed improved measurement method in gas-cell based miniature atomic clocks for better frequency stabilities. A simple light-shift measurement method using multiple photo-detectors (MPDs) suitable for chip-scale atomic clocks (CSACs) and miniature atomic clocks (MACs) has proposed [23]. A new observation method of Ramsey–coherent population trapping (CPT) characteristics has developed by employing different laser sideband combinations as the two interrogation pulses [24].

[References]

[1] N. Nemitz, T. Gotoh, F. Nakagawa, H. Ito, Y. Hanado, T. Ido, and H. Hachisu, "Absolute frequency of ^{87}Sr at 1.8×10^{-16} uncertainty by reference to remote primary frequency standards," Metrologia **58**, 025006 (2021).

[2] H. Hachisu, F. Nakagawa, Y. Hanado, and T. Ido, "Months-long real-time generation of a time scale based on an

optical clock," Sci. Rep. **8**, 4243 (2018).

[3] H. Hachisu, H. Ito, N. Nemitz, N. Ohtsubo, Y. Miyauchi, M. Morikawa, K. Matsubara, and T. Ido, "UTC(NICT) Referenced to a Timescale Based on the Optical Clock NICT-Sr1," in Proc. 2023 Joint Conference of the IEEE International Frequency Control Symposium and the European Frequency and Time Forum (IEEE IFCS-EFTF 2023) (in press).

[4] N. Ohtsubo, Y. Li, N. Nemitz, H. Hachisu, K. Matsubara, T. Ido, K. Hayasaka, "Frequency ratio of an ^{115}In+ ion clock and a ^{87}Sr optical lattice clock," Opt. Lett. **45**, 5950 (2020).

[5] M. Kajita and N. Kimura, "Prospects for vibrational transition frequency measurement of rare-gas hydride ions," J. Phys. Soc. Jpn. **90**, 044302 (2020).

[6] S. Nagano, M. Kumagai, H. Ito, Y. Hanado, and T. Ido, "Terahertz frequency counter based on a semiconductor-superlattice harmonic mixer with four-octave measurable bandwidth and 16-digit precision," Metrologia **58**, 055001 (2021).

[7] T. Kobayashi *et al*., Phys. Rev. Lett. **129**, 241301 (2022).

[8] M. Wada and H. Inaba. "Femtosecond-Comb Based 10 MHz-to-Optical Frequency Link with Uncertainty at the 10^{-18} Level." Metrologia **59**(6), 065005 (2022).

[9] N. Ohmae, M. Takamoto, Y. Takahashi, M. Kokubun, K. Araki, A. Hinton, I. Ushijima, T. Muramatsu, T. Furumiya, Y. Sakai, N. Moriya, N. Kamiya, K. Fujii, R. Muramatsu, T. Shiimado, and H. Katori, "Transportable Strontium Optical Lattice Clocks Operated Outside Laboratory at the Level of 10^{-18} Uncertainty," Adv. Quant. Tech. **4**, 2100015 (2021).

[10] Y. Tanaka, and H. Katori, "Exploring potential applications of optical lattice clocks in a plate subduction zone," J. Geod. **95**, 93 (2021).

[11] M. Takamoto, Y. Tanaka, and H. Katori, "A perspective on the future of transportable optical lattice clocks," Appl. Phys. Lett. **120**, 140502 (2022).

[12] H. Katori, "Longitudinal Ramsey spectroscopy of atoms for continuous operation of optical clocks," App. Phys. Exp. **14**, 072006 (2021).

[13] R. Takeuchi, H. Chiba, S. Okaba, M. Takamoto, S. Tsuji, and H. Katori, "Continuous outcoupling of ultracold strontium atoms combining three different traps," App. Phys. Exp. **16**, 042003 (2022).

[14] A. Yamaguchi, Y. Shigekawa, H. Haba, M. Wada, and H. Katori, "Laser spectroscopy of triply charged thorium ions towards a nuclear clock", SMI-2023, Giessen, Germany, May 8-11th, 2023.

[15] Y. Sugiyama, T. Kashimura, K. Kashimoto, D. Akamatsu, and F-L. Hong, "Precision dual-comb spectroscopy using wavelength-converted frequency combs with low repetition rates," Scientific Reports **13**, 2549 (2023).

[16] J. Nomura, T. Momma, Y. Kojima, Y. Hisai, T. Kobayashi, D. Akamatsu, and F-L. Hong, "Direct loading of Yb atoms into a 3D magneto-optical trap from a dispenser atomic source," AIP Advances **13**, 025361 (2023).

[17] Y. Tanabe, Y. Sakamoto, T. Kohno, D. Akamatsu, and F-L. Hong, "Frequency references based on molecular iodine for the study of Yb atoms using the $^1S_0 - {}^3P_1$ intercombination transition at 556 nm," Opt. Express **30**, 46487 (2022).

[18] Y. Kojima, K. Ikeda, Y. Tanabe, D. Akamatsu, and F-L. Hong, “Laser frequency measurement at the short-wavelength region using an intermediate laser and a frequency noise cancellation method," Opt. Lett. **47**, 30 (2022).

[19] K. Yoshida, M. Katagiri, H.-S. Jo, Y. Ueno, T. Morimoto, K. Sugiyama, Y. Imai, “Development of two single-ion spectroscopy system for the $^2S_{1/2} - {}^2D_{5/2}$ transition in ytterbium ions towards measurement of isotope shifts,” Joint Conference of the IEEE International Frequency Control Symposium and the European Frequency and Time Forum (IFCS-EFTF 2023), #7147 (2023).

[20] M. Mitaki and K. Sugiyama, “Phase-locking of octave-spanning optical frequency comb based on Kerr-lens mode-locked Yb:KYW laser to reference laser,” Jpn. J. Appl. Phys. **60**(2), 22003 (2021).

[21] K. Nakagawa, Development of transportable atomic gravimeters for field applications, 4th International Forum on Quantum Metrology and Sensing / QUANTUM INNOVATION 2021, Online, 8 December, 2021.

[22] T. Hojo, K. Takamura, K. Nakagawa, Development of highly sensitive gravimeter based on atom interferometry using hybrid system for field applications, 5th International Forum on Quantum Metrology and Sensing / QUANTUM INNOVATION 2022, Online, 29 November, 2022.

[23] M. Fukuoka, A. Hanatani and S. Goka, "Novel Light-shift Measurement Method with Multiple Photo Detectors for Gas-cell Based Atomic Clocks," 2022 Joint Conference of the European Frequency and Time Forum and IEEE International Frequency Control Symposium (EFTF/IFCS), doi: 10.1109/EFTF/IFCS54560.2022.9850834 (2022).

[24] M. Fukuoka and S. Goka, "Ramsey–CPT Resonance Observation Using Different Laser Sideband Combinations for the Two Interrogation Pulses," 2022 Joint Conference of the European Frequency and Time Forum and IEEE International Frequency Control Symposium (EFTF/IFCS), doi: 10.1109/EFTF/IFCS54560.2022.9850881 (2022).

A3. Realization of Electrical Unit (DC & LF)

A3.1 Josephson Voltage

A3.1.1 PJVS operation in dilution refregirator system

At NMIJ, A liquid-helium-free PJVS cooled with a GM cooler has been utilized since 2015 for calibrations of Zener voltage standards with the CMC values, 8 nV for 1 V and 45 nV for 10 V, same as those for their conventional JVS system cooled with liquid helium. They are now attempting to operate the PJVS chip on the 4 K stage in a dilution refrigerator system toward the quantum-metrology-triangle measurement and other general applications. Up to now, they have succeeded in the stable temperature control of the sample stages and the stable generation of the quantized voltage steps.

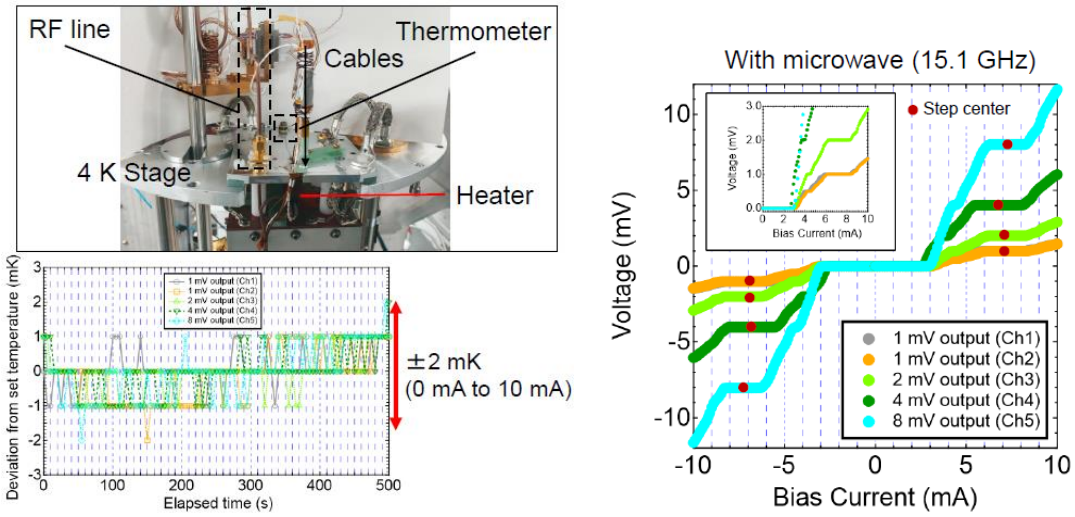

Fig.1 Implementation of PJVS module in a dilution refriqerator, temperature stability of 10 K stage, and quantized voltage steps generated from the PJVS.

A3.1.2 Thermodynamic temperature measurement

NMIJ measured the thermodynamic temperature of the melting point of gallium T_{Ga} using a Johnson noise thermometer (JNT) with an integrated quantum voltage noise source (IQVNS) as a reference. T_{Ga} was calculated using the fundamental constants recommended by the Committee on Data for Science and Technology (CODATA) for the revision of the International System of Units (SI). The measured T_{Ga} is consistent with the value defined in the International Temperature Scale of 1990. The power spectral density of output signal of IQVNS has been fixed so far. In order to use IQVNS as a reference for the measurement of thermodynamic temperature at various temperature fixed points, the power spectral density of the output signal of IQVNS should be variable. They improved part of the design of the device to be able to change the power spectral density of the output signal.

A3.2 Resistance

A3.2.1 Standard Resistors

At NMIJ, development of compact and ultra-stable 1 Ω and 1 kΩ standard resistors has been finished, and resistors with 10 kΩ are in progress of evaluation and development. The best resistors display extremely small average drift rates and temperature coefficients, and other performances, e.g.,

- 1 Ω: 4.2 nΩ/(Ω year), 4 nΩ/(Ω ˚C) at 23 ˚C,
- 10 Ω: 0.53 nΩ/(Ω year), 1 nΩ/(Ω ˚C) at 23 ˚C,
- 100 Ω: 50 nΩ/(Ω year), < 20 nΩ/(Ω ˚C) at 23 ˚C, deviation by transportation: < 10 nΩ/Ω, power and humidity coefficients are negligible,
- 1 kΩ: < 10 nΩ/(Ω year), 1.7 nΩ/(Ω ˚C) at 23 ◦C.

(note that the average drift rate and temperature coefficient of each resistance value does not come from the same resistor). It is demonstrated that this excellent performance is suitable for utilization in national metrology institutes and international comparisons.

Development of stable high-resistance standard resistors at NMIJ is also undergoing, and the developed resistors are now commercially available as type HVR10000 series from Japan Finechem corporation. The development is done mainly in 100 GΩ and the developed resistors show a small temperature coefficient of less than 5 (μΩ/Ω)/K and the other characteristics are also good.

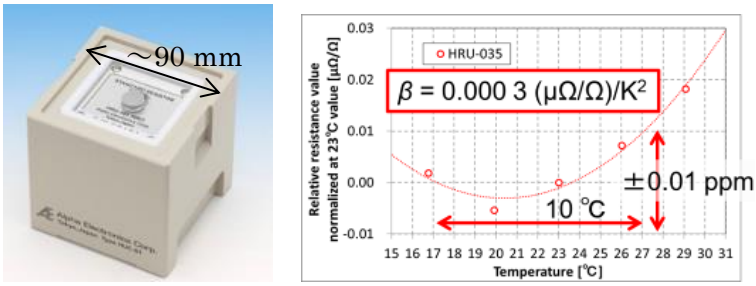

Fig. 2 Picture and temperature-resistance curve of developed 100 Ω standard resistor.

Fig. 3 Developed high-resistance standard resistor, HVR10000 series made by Japan Finechem corporation.

A3.2.2 DC high-resistance comparison between NIST and NMIJ

A precise high resistance comparison was performed between the traveling dual source bridge developed by NMIJ and the adapted Wheatstone bridge of the National Institute of Standards and Technology (NIST) from 10 MΩ to 100 TΩ at NIST. The NMIJ traveling bridge was shipped to NIST Gaithersburg and was installed right next to the NIST bridge and these bridges alternately measured the resistance ratio of the high resistance standards, without moving the location of the resistors inside the temperature controlled air-bath. Having the bridges and resistance standards in the same location for the comparison decreased the transportation and temperature coefficient effects on the resistance standards, contributing to the excellent agreement of the measured values. The NMIJ traveling bridge used an 8.5-digit digital multimeter and a relay switch box to determine a resistance ratio by measuring the ratio of the voltages applied to the resistors. The comparison was started from 10 MΩ based on the same 1 MΩ standard resistor calibrated using a NIST two-terminal cryogenic current comparator bridge, and standard resistors from 10 MΩ to 100 TΩ were calibrated by repeating 10: 1 scaling measurements with both systems. Excellent agreement was obtained within the uncertainty of all resistance ranges and the difference between both systems was less than 1 μΩ/Ω up to 1 TΩ and the degrees of equivalence for 10 TΩ and 100 TΩ were less than 6 μΩ/Ω [1].

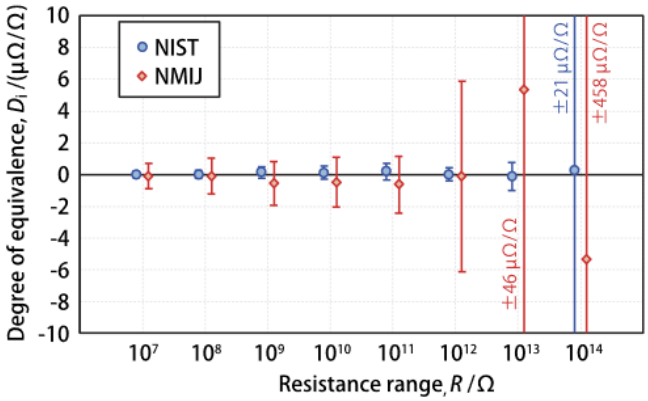

Fig. 4 .DoE for the measurements from 10 MΩ to 100 TΩ between NIST and NMIJ [1].

A3.2.3 Contact Resistance Evaluation of Wire Harness

To establish a relationship between the physical structure of electrical contact boundary and contact resistance, NMIJ developed a method for evaluating that using a physical simulated sample created via nanofabrication. Several samples with various distribution of “contact area” were made and their resistances were measured precisely. It was demonstrated experimentally that our result is in good agreement with an expression for constriction resistance.

Impedance measurement was introduced as a degradation diagnosis method for contacts of wire

harness by a nondestructive test. It was found that the changes in reactance at a certain frequency behave characteristically and independently of the DC resistance changes during accelerated test. The degradation degree of contacts was estimated by the change in impedance. (Contact: Yasuhiro Fukuyama, y.fukuyama@aist.go.jp).

A3.3 DC Current (single electron pumping)

Towards a realization of the current standard based on the single-electron pumping, NMIJ investigates the physics of low-temperature electron transport phenomena in various types of single-electron devices, i.e. superconductor-insulator-normal- insulator-superconductor (SINIS) turnstiles, gate-confined quantum dots, and graphene- or nanotube-based single-electron transistors. On SINIS turnstiles, in their early studies, they had discovered the new phenomenon that is a reduction of the single-electron pumping error induced by a weak magnetic field applied to the device. The origin of this phenomenon is related to the suppression of inverse-proximity effect at the interface between superconducting leads and a normal metal island. The inverse proximity effect causes the quasiparticle trap at the interface, namely it leads to the overheating of the junction. The magnetic field weaken the inverse proximity effect and helps to lease the quasiparticle. They justify this scenario from numerical analysis and controlling the tunnel resistance. Aiming at further reducing the pumping error, they extended the research to that based on another pumping mechanism. In one instance, they investigated a GaAs-based gate-defined quantum dot and demonstrated single-parameter pumping. In addition, they developed an air-bridge based parallel integration of this pump to demonstrate a synchronized parallel pumping that can generate a larger current otherwise unattained. In this study, they succeeded to operate the GaAs single electron device with sigma-delta modulated pulses for the arbitrary wave generation. This technique is thought to be useful for the calibration of current noise in the shot noise measurement. Also they start to measure the Si single electron pump device in collaboration with NTT group. At present they succeeded to operate single electron pumping at 1 GHz with 10^{-6}uncertainty. Also we are trying to operate this type of device in parallel to generate large (a few nano ampere) current. Four silicon pump devices are simultaneously operated at 1 GHz with 10^{-6} uncertainty levels inside dilution refrigerator. To test the uncertainty of pumped current, we are trying to compare the generated current each others. These single-electron devices are planned to be integrated with the quantum metrology triangle experiment that combine the single-electron device with the quantum Hall resistance and Josephson voltage standards. Towards this futuristic experiment, they had introduced a dry dilution refrigerator; An ample open space offered by this refrigerator allows them to integrate the whole components required for the triangle experiment including a cryogenic current comparator into one system. Electric noise filters and high-frequency wiring are now designed and constructed to complete this setup. Also to operate

Josephson voltage standard and quantum Hall array device inside the dilution refrigerator, they are installing additional cold stage and try to operate these quantum standards. As a result, they succeeded to operate Josephson voltage standard inside a dilution refrigerator. They obtained 1 V with 4.8×10^{-10} and 2 mV with 4.3×10^{-8}.

A3.4 LF-Impedance

At NMIJ, AC resistor calibration service has been kept in the range of 10 kΩ at 1 kHz. Standard capacitor (dry-nitrogen or used silica dielectric) calibration service has been kept in the range of 10 pF up to 1000 pF at 1.592 kHz. They have started a development of precision measuring techniques for diagnosis of the energy storage devices such as lithium-ion batteries and super-capacitors by using an impedance spectroscopy method. They have a plan to establish a metrology for evaluating the storage power devices. Preliminary impedance measurements for lithium-ion battery cells in the range of 10 mHz – 10 kHz demonstrated that the impedance value for unused cells is clearly distinguished from that for used-up cells. Impedance spectra for the unused cells which are obtained under 100 mΩ indicate that the evaluations of the uncertainties should be required for detecting a faint sign or a symptom of degradations of storage devices. They have developed an electrochemical impedance measurement system and have evaluated the type-A uncertainty for the impedance spectra which was estimated to be less than 0.2 mΩ.

National institute of Advanced Industrial Science and Technology (AIST) established the Global Zero Emission Research Center (GZR) in 2020. GZR has a mission for an international joint research base for zero emission technologies. GZR started to research for innovative environmental and energy technologies, including in the fields of renewable energy, storage batteries, hydrogen, and so on. NMIJ joined in GZR and has started the research of the safety and reliability evaluation method for solid oxide electrochemical cells and lithium ion batteries by using precision impedance and charge-discharge measurements.

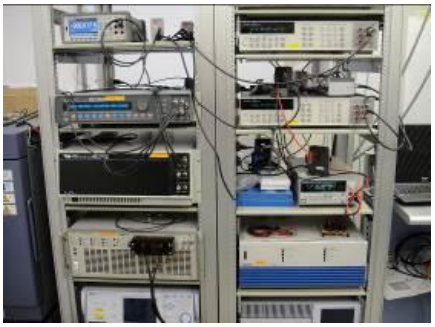

Fig. 5 Photograph of the electrochemical impedance measurement system developed using the Frequency Response Analyzer and the Potentio-Galvano Stat.

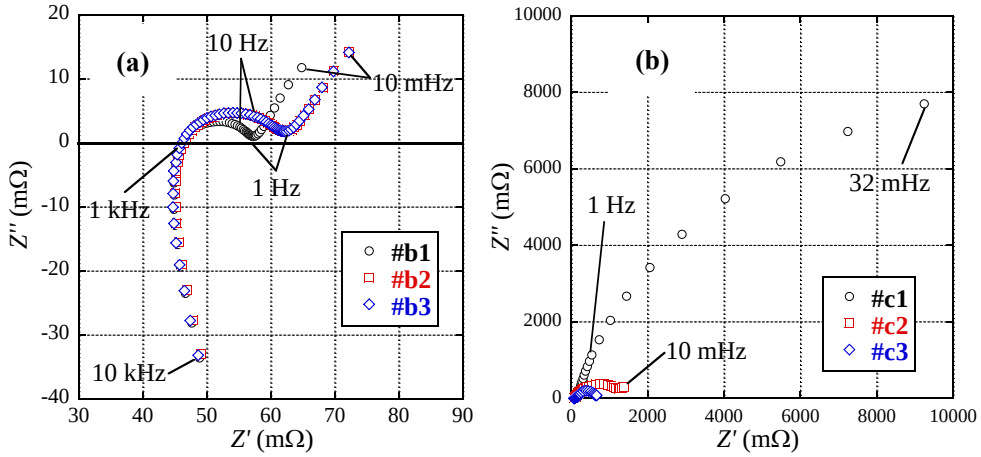

Fig. 6 Nyquist plot of the impedance spectra for the 18650-type lithium-ion batteries: (a) the unused samples and (b) used-up samples. Obvious change in impedance spectra was observed with the progression of the charge/discharge cycle.

A3.5 AC/DC transfer

NMIJ has provided ac-dc voltage difference transfer calibration of thermal converters in the voltage range from 10 mV to 1000 V and in the frequency range from 10 Hz to 1 MHz, and AC voltage calibration below 10 Hz. They have been participating in APMP. EM-K12 comparison [2], and CCEM-K6a/K9 key comparison [3]. The thin film multi-junction thermal converters with a novel design have been developed in collaboration with NIKKOHM co. ltd. We have introduced a new thermopile pattern to improve the performance of their thin film MJTC [4]. Using these thermal converters, novel thermal converter circuits arranged in an 2 by 2 matrix have been fabricated to improve the low-frequency AC-DC transfer differences [5]. Thin-film AC-DC resistor on an aluminum nitride (AlN) substrate with negligible voltage dependence have been fabricated for measuring AC voltages up to 1000 V [6]. Toward next-generation AC/DC current transfer standard, high-current multijunction thermal converters on a Si substrate up to 1 A have been designed and fabricated through the collaborative project with National Institute of Standards and Technology in Gaithersburg [7].

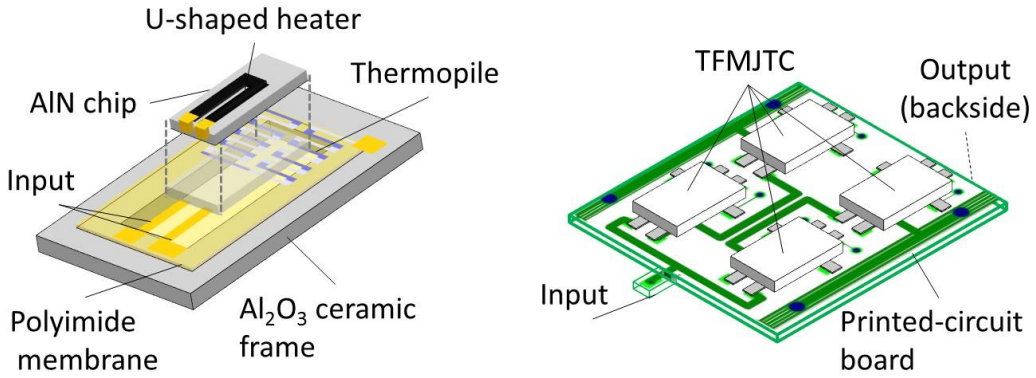

Fig. 7

Toward quantum AC voltage standards, a differential sampling measurement system using an AC-programmable Josephson voltage standard (AC-PJVS) system has been developed at NMIJ [8]. To extend the voltage range of the system, they have combined a two-stage inductive voltage divider and an 10 V AC-programmable Josephson voltage standard chip.

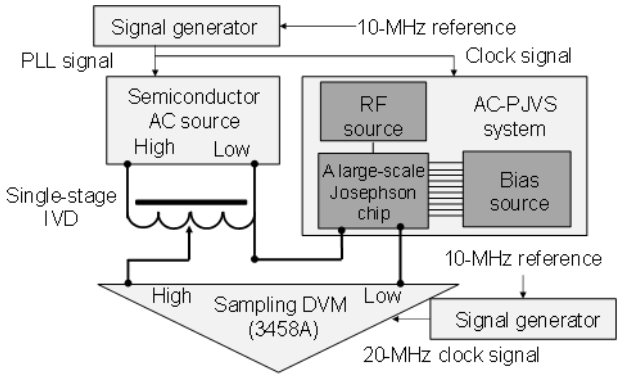

Fig. 8

Toward a waste-heat recovery with thermoelectric conversion, they have developed advanced metrology techniques and apparatus using a precise ac and dc electrical measurement technique. The Seebeck coefficient is an essential indicator of the conversion efficiency and the most widely measured property specific to these materials. So far, they have developed a method to precisely measure Thomson effect to determine the absolute Seebeck coefficient of platinum reference material [9,10].

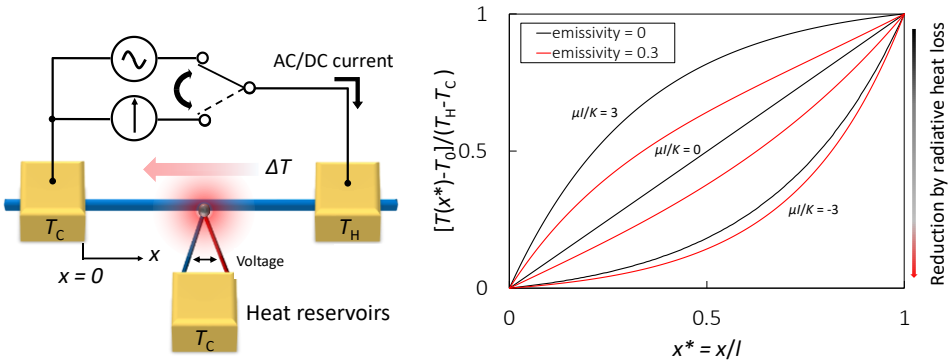

Fig. 9

A3.6 Power

An improved evaluation system for a wideband resistive voltage divider (WRVD) is under development at NMIJ. The fabrication of an accurate and precise WRVD based on the extended Hamon method has been realized by direct soldering of series resistor and by soldering on the edge of round substrates for parallel resistor with suitable fixtures. The improved evaluation system was verified with calibrated IVDs. By replacing with a phase standard, the difference from the calibration result by Thompson's method has been effectively reduced comparing with the previous system. An error simulation of the equivalent circuit of the IVDs based on the calibration result has revealed the large quadrature error of the improved system at 50 kHz. It was considered due to the phase error of the phase standard.

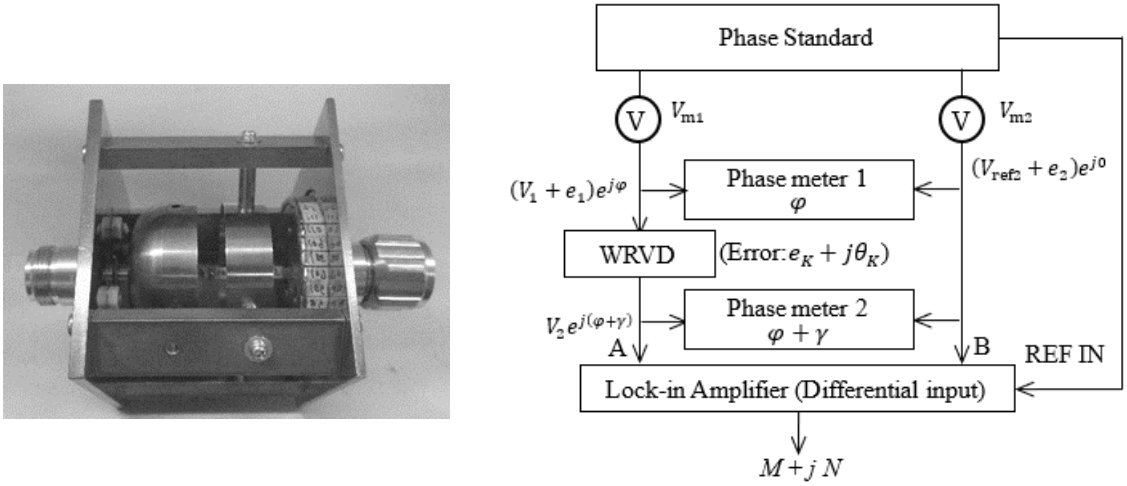

Fig. 10

[References]

[1] T. Oe, S. Payagala, A. R. Panna, S. Takada, N.-H. Kaneko, and D. G. Jarrett, "Precise high resistance comparison between the NMIJ traveling dual source bridge and the NIST adapted Wheatstone bridge," Metrologia **59**(6),

065007 (2022).

[2] APMP. EM-K12, Key comparison of AC-DC current transfer standards. (https://www1.bipm.org/kcdb/comparison?id=509)

[3] CCEM-K6.a/K9, CIPM Key Comparison of AC-DC Voltage Transfer Standards.

[4] H. Fujiki, Y. Amagai, K. Shimizume, K. Kishino, S. Hidaka, “Fabrication of Thin Film Multijunction Thermal Converters With Improved Long-Term Stability,” IEEE. Trans. Instrum. Meas. **64**(6) (2015).

[5] Y. Amagai, H. Fujiki, K. Okawa, N.-H. Kaneko, “Low-Frequency AC–DC Differences of a Series–Parallel Circuit of Thermal Converters,” IEEE. Trans. Instrum. Meas. **68**(6) (2019).

[6] H. Fujiki, Y. Amagai, and K. Okawa, “Establishment of High-Voltage AC–DC Voltage Transfer Standards in 1–100-kHz Range at NMIJ,” IEEE. Trans. Instrum. Meas. **68**(6) (2019).

[7] Y. Amagai, S. Cular. J. A. Hagmann, T. E. Lipe, N.-H. Kaneko “Low-Frequency Characteristics of Silicon-Based High-Current Multijunction Thermal Current Converters Fabricated by Wet Chemical Etching” IEEE. Trans. Instrum. Meas. **70** (2021).

[8] Y. Amagai, M. Maruyama, H. Yamamori, T. Shimazaki, K. Okawa, H. Fujiki, and N.-H. Kaneko, “Extending voltage range to 10 V rms in AC–DC difference measurements with AC programmable Josephson voltage standard” Meas. Sci. Technol. **31**, 065010 (2020).

[9] Y. Amagai, T. Shimazaki, K. Okawa, T. Kawae, H. Fujiki, and N.-H. Kaneko, “High-accuracy compensation of radiative heat loss in Thomson coefficient measurement,” Appl. Phys. Lett. **117**, 063903 (2020).

[10] Y. Amagai, T. Shimazaki, K. Okawa, T. Kawae, H. Fujiki, and N.-H. Kaneko, “Precise absolute Seebeck coefficient measurement and uncertainty analysis using high- T_c superconductors as a reference,” Rev. Sci. Instrum. **91**, 14903 (2020).

A4. EM Field, Power Density and Antenna Measurement

Calibration service at NMIJ for the free-space antenna factor of loop antenna is available in the frequency range of 20 Hz to 30 MHz. The expanded uncertainty of the magnetic antenna factor is from 0.4 dB to 0.7 dB in the frequency range from 9 kHz to 30 MHz [1]. As a result of the improvement mentioned above, NICT started to provide the magnetic-field antenna factor of loop antennas with lower expanded uncertainty than before since June 2023. In addition, two kinds of loop antenna calibration methods developed by NMIJ and NICT are standardized by IEC/CISPR (International Special Committee on Radio Interference) in 2022 [2].

AC Magnetic field sensor evaluation service at NMIJ is available in a range of 1 μT to 150 μT from 50 Hz to 100 kHz. The realizable field strength depends on frequency points [3].

Novel EM-sensor and an EM visualization method by using quantum phenomena of vapor cesium atoms are currently under development at NMIJ [4-6].

At NMIJ, calibration of the dipole antenna factor above a ground plane from 30 MHz to 1 GHz in the specific conditions (with horizontal polarization at 2.0 m from the ground plane surface) is available. Since EMC (electromagnetic compatibility) measurements are ordinarily carried out in free space above 1 GHz, the dipole antenna factor from 1 GHz to 2 GHz is calibrated in an anechoic chamber. The free space dipole factor is one of the traceability sources of the E-field strength calibration in free space. The free space antenna factor calibration services for broadband antenna for Biconical antenna (30 MHz to 300 MHz), Log periodic dipole array antenna (300 MHz to 1000 MHz) and Super broadband antenna (30 MHz to 1000 MHz) are being performed using their original three antenna calibration method. In 2022, calibration certificates for broadband antennas were digitized. Four digitized calibration certificates (DCCs) were issued in December 2022. An antenna factor calibration service for the broadband horn antenna (1 GHz to 18 GHz) is available using the time-domain single antenna extrapolation method in the semi-anechoic chamber [7, 8]. An antenna gain calibration service for millimeter-wave standard gain horn antenna are being performed form 50 GHz to 110 GHz and 220 GHz to 330 GHz using a time-domain processing and extrapolation technique. Compact antenna test range for 6G wireless system (the frequency range of 110 GHz to 330 GHz) are now developing using offset Gregorian type parabolic reflector (Fig.11) This system will be able to evaluate sub-THz antenna radiation pattern and also RCS pattern of RIS (Reconfigurable Intelligent Surface) for improving 6G radio propagation environment.

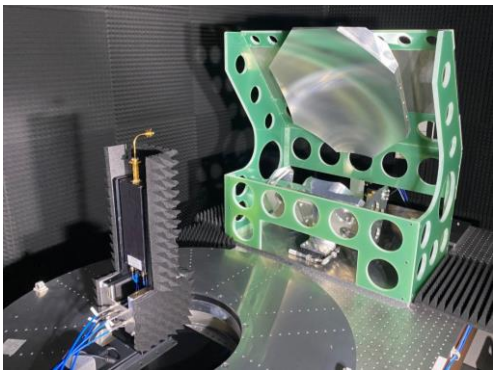

Fig.11. Offset Gregorian type parabolic reflector for evaluating 6G sub-THz antenna and RIS.

The E-field strength is one of the important quantities in the electromagnetic free field metrology and the E-field is ordinarily measured by using a calibrated field probe. At NMIJ/AIST, the correction factors of the E-field probe are calibrated against the standard field levels of 10 V/m and 20 V/m generated in a G-TEM cell. Three appropriate methods to generate standard E-field are employed in calibrating the response of the primary optical field transfer probe depending on the measurement frequency. A TEM cell is employed as a standard E-field generator at lower frequencies below 900 MHz, and the E-field level generated in the anechoic chamber from 0.8 GHz to 2.2 GHz is calibrated by using the free space dipole antenna factor and measured power at the antenna port. Transmitting antenna gain and the net power flowing into the antenna are the traceability sources for the standard field from 2 GHz to 4 GHz. The optical E-field transfer probe calibrated against these standard E-fields transfers the E-field level into the G-TEM cell, and then the ordinary field probe is calibrated [9].

NICT performs the calibration service for frequency standard, RF measurement instruments such as RF power meters, RF attenuators, DC/AC calibrators, DMM and antennas to maintain the radio station licensing system according with the radio low in Japan. Especially, calibration service of RF power meters in the frequency range up to 330 GHz has been available since 2021. The initial purpose of the service was spurious measurements in accordance with the ITU-R recommendation SM.32-10, however, it contributes to licensing to radio stations using 300 GHz band, too. It has been worked out by a collaboration between NICT and NMIJ.

For electromagnetic interference (EMI) measurements in the frequency range below 30 MHz, a test site validation method was developed by NICT [10, 11]. The method was standardized by IEC/CISPR [12]. In addition, NICT also contributed to determination the compliance test method standardized by IEC/CISPR [13].

[References]

[1] M. Ishii, “Improvement of Uncertainty in Calibrating Primary Standard Loop Antenna by Three-antenna Method,”

2022 Conference on Precision Electromagnetic Measurements (CPEM) (2022).

[2] IEC/CISPR, Specification for radio disturbance and immunity measuring apparatus and methods - Part 1-6: Radio disturbance and immunity measuring apparatus - EMC antenna calibration, edition 1.2 (CISPR 16-1-6, Ed.1.2) (2022).

[3] M. Ishii and M. Suzuki, “Impedance of Helmholtz Coils to Generate Standard AC Magnetic Fields in High Frequency,” 2020 Conference on Precision Electromagnetic Measurements (CPEM) (2020).

[4] M. Ishii, “A study of frequency extension of AC magnetic field sensor using radio-optical multiple resonance in ^{133}Cs,” EMC europe 2020 (2020).

[5] M. Ishii and M. Kinoshita, “A feasibility study of a real-time visualization method for electromagnetic fields,” Microw. Opt. Technol. Lett. **63**, 399-403 (2021).

[6] M. Ishii, “A Feasibility Study of AC Magnetic Field Sensor in kHz-band Based on Quantum Phenomena in ^{133}Cs,” 2022 Conference on Precision Electromagnetic Measurements (CPEM) (2022).

[7] Y. She, S. Matsukawa, S. Kurokawa, "Uncertainty Analysis of Far-Field Gain Measuement of DRGH Using Single-Antenna Extrapolation Method from 1 GHz to 18 GHz," 2022 MJWRT, Malaysia, (Hybrid workshop) (2022).

[8] Y. She, S. Matsukawa, "A measurement test for antenna alignment using image processing and uncertainty estimation, " IEICE Communications Express **12**(6), 260–264 (2023).

[9] T. Morioka, "Systematic and random errors in the net power measurement using a reflectometer," IEEE Trans. Instrum. Meas. **70**, 1010110 (2021).

[10] K. Fujii, “Basic characteristics of magnetic field antenna factor of loop antennas for EMI measurement,” IEICE Communications Express **11**(10), 643-648 (2022).

[11] K. Fujii, “Effects of feed gap arrangements of loop antennas on site validation for EMI measurements below 30 MHz,” IEICE Communications Express **11**(11), 721-726 (2022).

[12] IEC/CISPR, Specification for radio disturbance and immunity measuring apparatus and methods - Part 1-4: Radio disturbance and immunity measuring apparatus - Antennas and test sites for radiated disturbance measurements, edition 4.2 (2023).

[13] IEC/CISPR, Specification for radio disturbance and immunity measuring apparatus and methods - Part 2-3: Methods of measurement of disturbances and immunity - Radiated disturbance measurements, edition 4.2, (2023).

A5. Power Attenuation and Impedance Measurements

A5.1 RF-Power

NMIJ developed a WR-5 waveguide-based calorimeter for the frequency range of 140-220 GHz in collaboration with NICT. Direct comparison calibration was demonstrated for commercially available power meters using the calorimeter as a reference standard. We have begun to provide reference values for the WR-5 band to domestic organizations.

A5.2 RF-Attenuation and Phase Shift

NMIJ has established national standard for RF and microwave attenuation in the frequency range of 1 kHz to 110 GHz, and provides its calibration services mainly with the Japan Calibration Service System (JCSS) scheme. All measurement and calibration systems work based on the intermediate frequency (IF) substitution method using the highly accurate null detection and employing an inductive voltage divider (IVD) as the reference standard. A recent improvement was the inclusion of a new measurement system in the frequency range of 1 kHz to 100 kHz, as shown in Fig. 12 to meet industry requirements for electromagnetic compatibility (EMC) [1]. These systems have been commercially manufactured by 7Gaa Corporation (https://7gaa.co.jp/) and several have been shipped to overseas NMIs for use as their national RF attenuation standards.

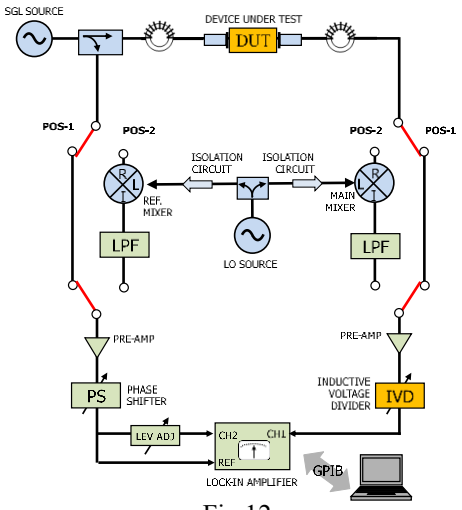

Fig.12

NMIJ established national standard for RF phase shift in the frequency range of 10 MHz to 1 GHz. The expanded uncertainties are 0.029° for DUT with losses up to 20 dB, 0.031° for 40 dB, and 0.056° for 60 dB loss. The frequency range is currently being expanded to 18 GHz [2, 3].

NMIJ took an initiative to organize a CIPM Key Comparison of attenuation at 18 GHz, 26.5 GHz and 40 GHz using a step attenuator (CCEM.RF-K26) [4]. Measurements of both the first and second round loop were completed in February 2018. It can be said successful, although there were some delays in the delivery of the traveling standards between the participants. The Draft B Report is currently under review by the CCEM members.

A5.3 RF-Impedance and related measurement technology

NMIJ researched the precision on-wafer measurement techniques over 100 GHz and developed a full-automatic RF probing system establishing high reproducibility of measurements. Balanced type circular disk resonator method has been developped and commarcialized, in addition, the

method will be published as an IEC standardization. The method cannot only measure dielectric permittivity but also conductivity at millimeter wave frequency (Fig.13). Furthermore, electromagnetic sensing techniques is also researching for the agriculture products, food and infrastructure, etc.

NMIJ as a pilot laboratory is managing the CCEM key comparison (CCEM.RF-K5c.CL: S-parameter for PC3.5 in the range from 50 MHz to 33 GHz) [5], the APMP supplemental comparison (APMP.EM.RF-S5.CL: Dimensionally-derived characteristic impedance for PC7, PC2.4 and PC1.85) [6] and the pilot study for material characterization.

Calibration certificates for S-parameter measurements using the vector network analyzers have been digitized at NMIJ. Six calibration certificates were issued in November 2022.

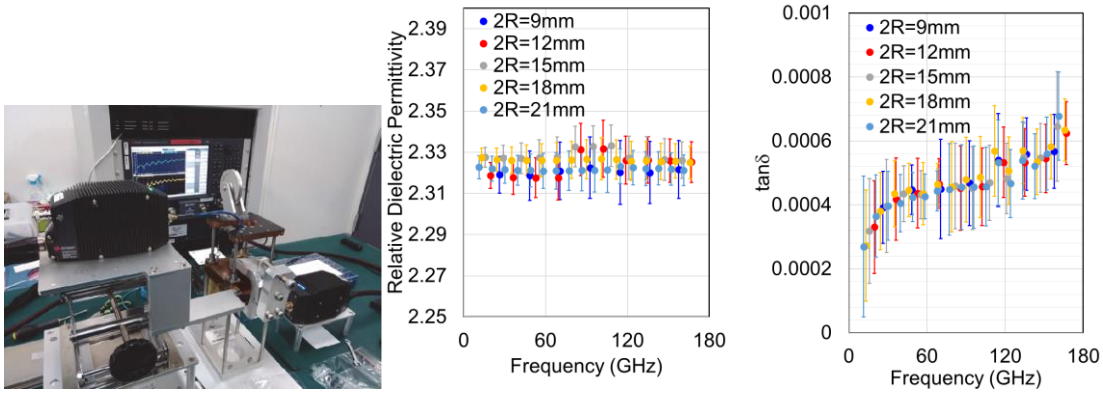

Fig. 13 Balanced type circular disk resonator at millimeterwave frequency

A5.4 Terahertz Metrology

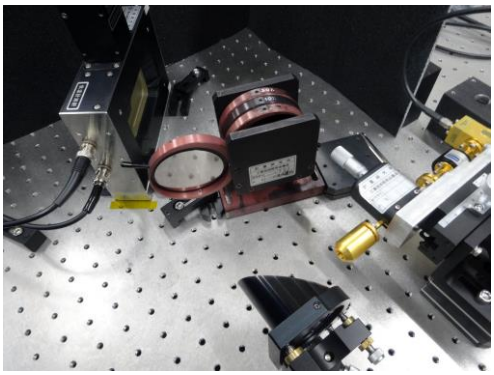

Fig. 14 Photograph of the THz attenuation calibration system for free-space beams.

NMIJ developed a method for measuring terahertz (THz) attenuation for free-space beams (Fig. 14). It employs a photo-acoustic detector to compare THz attenuation to audio-frequency (AF) attenuation. The AF attenuation is directly calibrated by an inductive voltage divider as a reference standard. Using a metalized-film attenuator, we have demonstrated attenuation measurements up

to 20 dB for 0.11 THz collimated beams.

A5.5 Material Characterization

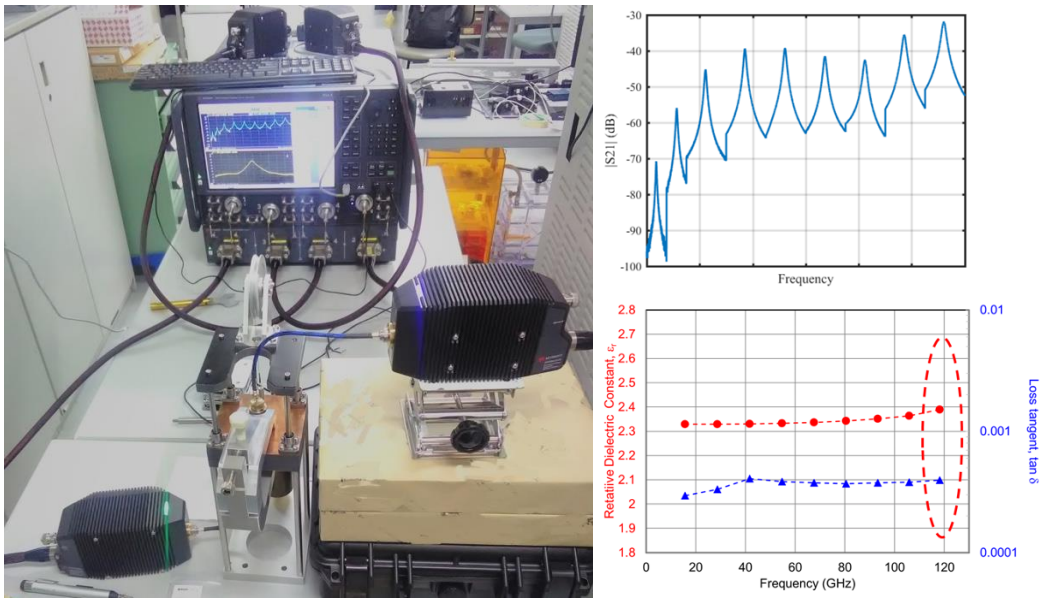

Fig. 15 Photographs of Balanced-type circular-disk resonator(BCDR) and Measurement Results of cyclic olefin polymers (COP) up to 120 GHz

NMIJ is researching and develops material characterization, i.e. dielectric permittivity measurements, at the millimeterwave frequency. NMIJ developed the Balanced-type circular-disk resonator (BCDR) and analytical software for dielectric permittivity of low loss materials. Measurement can be performed in broad band frequency and up to 120 GHz (Fig. 15). The method is now being standardized in the IEC standard, then the system has been provided by the measurement instrument company. Furthermore, NMIJ as a pilot laboratory manages the Pilot study for dielectric permittivity measurement proposed by NIST as a former pilot laboratory in it.

[References]

[1] A. Widarta, "Primary standard of attenuation in the frequency range of 1 kHz to 10 MHz," in CPEM Dig., Denver, Co, Aug. 2020, virtual.

[2] A. Widarta, "Precision phase shift measurement system in the frequency range of 1-18 GHz," 50th European Microwave Conf., Utrecht, The Netherlands, Jan. 2021, virtual.

[3] A. Widarta, "Working Standard for RF Attenuation and Phase-shift Calibrations," in CPEM Dig., Wellington, NZ, Dec. 2022.

[4] https://www.bipm.org/kcdb/comparison?id=1016

[5] https://www.bipm.org/kcdb/comparison?id=599

[6] https://www.bipm.org/kcdb/comparison?id=333